SSRG International Journal of Electrical and Electronics Engineering
ISSN: 2348-8379/ https://doi.org/10.14445/23488379/IJEEE-V11I12P137

Volume 11 Issue 12, 406-413, December 2024

Original Article

Multi-slot Terahertz Triangular Shaped Antennas for 6G Communication System

Siddalingappagouda Biradar[1], Vinod B. Durdi[2], M.G. Shalini[3]

[1,3]Department of Electronics and Communication Engineering, Dayananda Sagar Academy of Technology, Karnataka, India.
[2]Department of Electronics and Telecommunication Engineering, Dayananda Sagar College of Engineering, Karnataka, India.

[1]Corresponding Author : siddubiradarr@gmail.com

Received: 21 October 2024 Revised: 22 November 2024 Accepted: 20 December 2024 Published: 31 December 2024

***Abstract* -** *The new upcoming 6th Generation (6G) communication marks a significant advancement in wireless and mobile networks, and it is expected to provide speeds that are potentially 100 times faster than the 5th Generation (5G) technology while offering extremely low delays, high data transfer, and enabling numerous devices to connect. The terahertz communicating antennas are the crucial components for high-speed communication systems, which offer extended coverage, high beam, directivity, and gain at wavelengths between 3 mm and 30 µm. In this paper, a novel multi-slot triangular copper microstrip patch antenna is designed with an operating frequency ranging from 1 THz to 5 THz. The antenna is designed, simulated, and analyzed using the Computer Simulated Technology (CST) studio suite, and the design consists of a microstrip patch, feedline, substrate, and ground plane. The simulation parameters, such as S-parameter, VSWR, resonant frequency, bandwidth, gain, electric and magnetic field, surface current, and diversity, are calculated. The simulation results of the proposed antenna predict the best suitability for the 6G communication system.*

***Keywords* -** *Microstrip patch antennas, Feedline, Substrate, Ground plate, 6G communication system.*

1. Introduction

As society increasingly adopts the capabilities of generation technology known as 5G, planning is already proceeding for the next major advancement in communication technology, the introduction of 6G networks. If we believe that 5G is groundbreaking and robust in its capabilities. The anticipation is that 6G will be a game-changer in a shift of proportions to redefine connectivity and significantly impact our life dynamics, including how we communicate and engage with our environment. The paper [1] has an antenna dimension of 160×120 µm² with a resonating frequency of 2.68 THz simulated using the CST tool and has a return loss of -33.22 dB, 7.72 dB of gain, a wide bandwidth of 1.27 THz, and 95.32% efficiency.

The materials used for design are copper (ground plane and patch antenna) and FR4 (as a substrate plane). This triangular-shaped antenna is suitable for terahertz applications. In work carried out in the paper [2], the antenna is designed with dimensions of 63.8x60x1.6 mm³ and the material used is copper (ground plane and patch antenna) and FR4 (as a substrate plane) simulated using the CST tool; the simulation results of the copper patch antenna has a reflection co-efficient of -18 dB, a bandwidth of 2.41 GHz, less than 2 values of VSWR, and has a maximum gain of 4 dB. The antenna simulation results define it as being suitable for wireless S-band applications. In the research work in the paper [3], the microstrip triangular patch antenna is designed with a resonating frequency of 5.44 GHz simulated using the HFSS simulation tool, and the simulation results of the antenna is of gain 12.10 dB, return loss of -22 dB with an efficiency of 84.2%. This high-gain 5G antenna is used for long-distance communication, IoT and smart cities, broadcasting, and military and defense applications.

In the simulation in the paper [4], the arc-shaped slotted triangular microstrip patch antenna is simulated using HFSS and CST tools; the substrate material used is Rogers TMM4 and copper material for the patch and ground plane. The antenna resonates at 3.3 GHz and has a return loss of -26.53 dB with a maximum gain of 6.5 dBi. The paper [5], with the dimension of 47.46*44.84 mm², multiband antenna designed and simulated using the CST tool with a 3.15 GHz resonating frequency, has a directivity of 9.82 dBi and a gain of 8.99 dBi. This antenna can be used for 5G and satellite communication. In the paper [6], the dimension of the T-shaped microstrip patch antenna is 30.9×26.63×0.1 mm³, operates between 4 GHz and 16 GHz and is simulated using the CST tool. The antenna produces a simulation result of a maximum gain of 7.99 dBi at 15.35 GHz and a return loss of -31.01 dBi at 8.43 GHz. The material used for the substrate is Rogers 5880, and copper is for the antenna area and ground plane.

Table 1. Comparison table

Ref. No.	Design Area (L*W*H) mm	Resonating Frequency (GHz)	Gain (dBi)	Substrate Material	Shape	S-Parameter (dB)	Tool Used
[7]	25*22*1.6	5.79	1.49	FR4	Slotted Triangular	-24.95	CST
[8]	40*35	7.21	8	FR4	Slotted Triangular	-24.12	HFSS
[9]	56*48	2.96	4.32	FR4	Slotted Triangular	-20.11	CST
[10]	20*18	4.46	3.79	FR4	Slotted Triangular	-11.89	CST
[11]	35*25*1.57	26	7.47	RDuroid 5880	Slotted Triangular	−30.70	CST
[12]	7.23*6.28*0.5	28	8.35	RT/Duroid 5880	Slotted Triangular	-18.11	HFSS
[13]	100*100*1.52	5.71	4.37	Rogers RT 6202	Slotted Triangular	-33.12	CST
[14]	50*60*1	2.46	3	FR4	Slotted Triangular	-17	CST
[15]	50*50*30	3.54	7.29	RTDuriod-5880	Slotted Triangular	-10	HFSS
[16]	30*20*0.8	6.85	4.46	FR4	Slotted Triangular	-16.11	HFSS
Proposed	64.5*64.5*1.6μm	3.16THz	8.43	FR4	Slotted Triangular	-35.96	CST

2. Design and Simulation Parameters

This section shows the proposed multi-slot terahertz triangular-shaped antennas in Figures 1 (a), (b), (c), and (d). These triangular antennas have no slots or some slots in them. The length and width of the substrate and ground plane are the same. The patch and ground plane material is copper; the substrate is FR-4 (lossy).

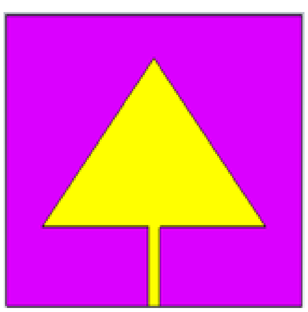

Fig. 1(a) No slot

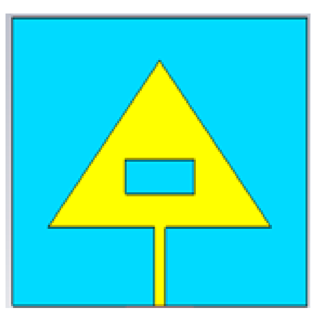

Fig. 1(b) Single slot

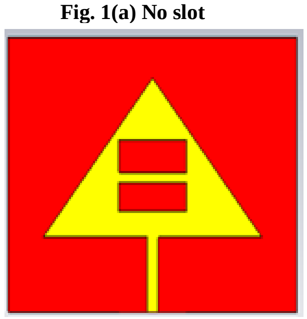

Fig. 1(c) Double slot

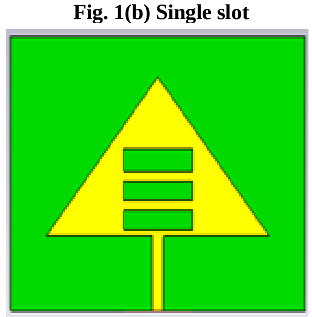

Fig. 1(d) Triple slot

The FR-4 material is most commonly used for substrate planes because of its cost-effectiveness and versatility. It is a more convenient choice for antenna fabrication, and it has brilliant mechanical strength and is robust, making it appropriate for applications requiring durable antennas. FR-4 is well-suited to PCB manufacturing techniques, allowing easy and precise fabrication of microstrip patch antennas, arrays, and other designs. It is a flame-retardant material, reducing the risks in critical environments. Copper is most commonly used for 5G and 6G antennas because of its excellent electrical and physical properties. Copper provides high electrical conductivity, low signal attenuation, better durability and mechanical strength, and excellent thermal conductivity. The triangular slotted microstrip patch antenna is unique; the presence of slots or cuts introduced into the patch can significantly impact the antenna's characteristics. The presence of slots can increase the length of the current path, thereby broadening the antenna's bandwidth.

Table 2. Parameters used for microstrip patch antenna

Sl. No.	Parameters		Values (μm)
1	Wf	Feedline Width	4.8
2	Hs	Feedline Length	22.8
3	Wg	Ground Width	64.5
4	Lg	Ground Length	64.5
5	Hg	Ground Height	1.6
6	Ws	Substrate Width	64.5
7	Ls	Substrate Length	64.5
8	Hs	Substrate Height	1.6

This also helps to resonate the antenna at multiple frequencies. Slots can modify the input impedance of the antenna, allowing better matching to the feeding network. This reduces antenna reflection losses and improves efficiency. Slots can lead to control of the current spreading on the patch, providing desired radiation patterns, higher directivity, and lower sidelobe levels. This is critical for beamforming in 5G/6G antenna arrays. The slots' shape, size, and location can be adjusted to fine-tune the antenna's resonant frequency. The presence of a slot also offers design changes to meet specific frequency requirements. The flow chart of antenna design, as shown in Figure 2, shows the step-by-step procedure for designing a patch antenna. The initial step defines the project goal: antenna type, frequency band, and application.

Launch CST and create a new project. Set the design frequency, choose the appropriate material, and define its simulation variables: thickness, loss tangent, and dielectric constant. The second step is to design an antenna by defining the proper geometry of the antenna (length, width, and slots) and setting the size and structure of the feedline, ground plane, substrate, and patch plane. The third step is to set the boundary conditions and excitation type. The fourth step is to start the simulation and check the simulation results (S-parameter, VSWR, efficiency, bandwidth, gain, and directivity) to estimate the antenna performance. The fifth step is to modify the design (like adjusting the patch dimensions, antenna slot positions, substrate properties, or feedline structure) according to the results to meet the required specifications.

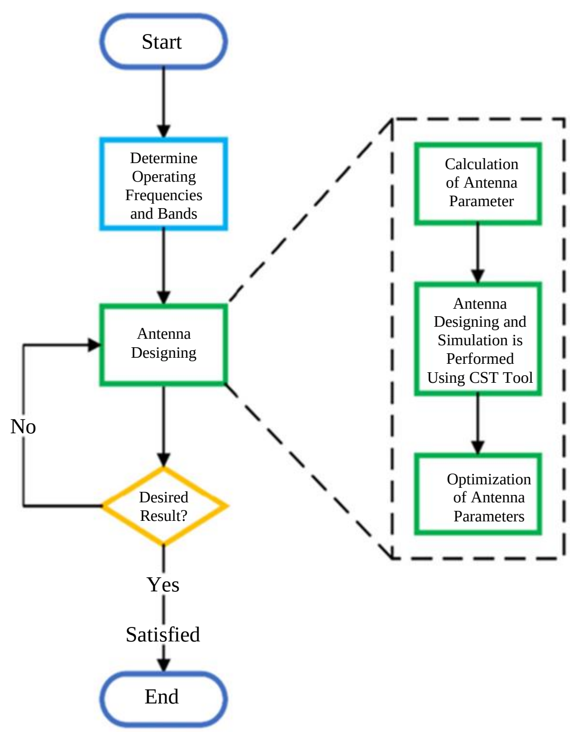

Fig. 2 Flowchart of antenna design

The last step is to confirm the final design by re-simulating and performing over the desired frequency range. The frequency range from 1 THz to 5 THz balances penetration depth, resolution, and sensitivity, making it invaluable for various scientific, medical, and industrial applications.

3. Results and Discussion

3.1. Return Loss

It measures the reflected wave or signal strength travelling or returning to a transmitter from an antenna. It is called the reflection coefficient or scattering parameter (S11), one of the critical parameters. For 6G antennas, the S11 value should be less than -10 dB, corresponding to 10% of the power being reflected and 90% being transmitted. If the value is between -15 dB and -20 dB or lower, it corresponds to even less reflection and more efficient power transmission. Table 3 shows the return loss or reflection coefficient with and without slots in the antenna. As the number of slots increases, the reflection co-efficient decreases and bandwidth increases. The slots can increase the effective length of the current path, thereby increasing the antenna's bandwidth. The above simulation results from Figure 3 confirm that the three-slot triangular antenna with a frequency of 3.16 THz has less than 2% return loss being reflected. The no slot, single and double slot antenna with 4.30 THz, 1.25 THz, and 2.11 THz has less than 3% return loss.

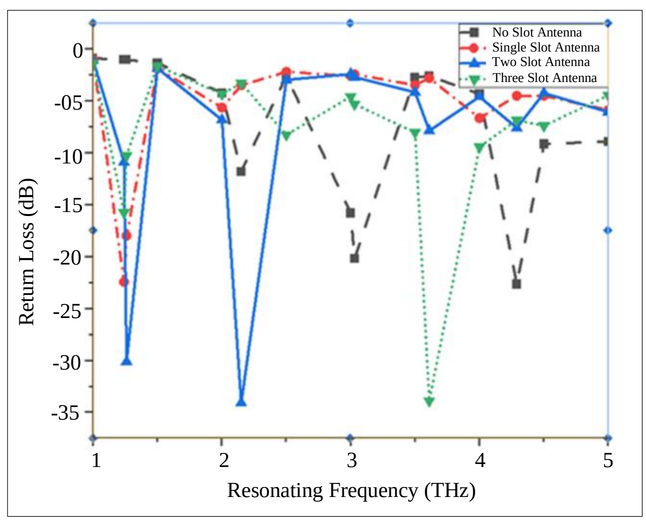

Fig. 3 Graph of return loss versus resonating frequency of the triangular shaped antenna

Table 3. Return loss of triangular shaped antenna

Sl No.	Triangular Antennas	Frequency (THz)	Return Loss (dB)	Bandwidth (GHz)
1	No Slot	4.30	-22.43	21
2	Single Slot	1.25	-22.48	7
3	Double Slot	2.11	-34.17	14
4	**Three Slot**	**3.16**	**-35.96**	**20**

3.2. Voltage Standing Wave Ratio (VSWR)

This simulation metric defines how well the antenna is impedance-matched to the transmission line or source. The VSWR value is directly related to return loss, with a lesser VSWR value indicating better impedance matching, introducing additional resonances and reduced power reflection.

For 6G antennas, the VSWR should be 2:1, indicating less than 4% power reflection and better impedance matching.

The simulation results from Figures 7, 8, 9, and 10 show that a three-slot triangular microstrip patch antenna with a frequency of 3.16 THz has a lower value of 1.03.

The no slot, single, and double slot antennas with frequencies of 4.30 THz, 1.25 THz, and 2.11 THz have VSWR values of 1.16, 2.11, and 1.04, respectively.

This ensures that a three-slot triangular antenna has better impedance matching, lesser power losses, and improved overall antenna efficiency.

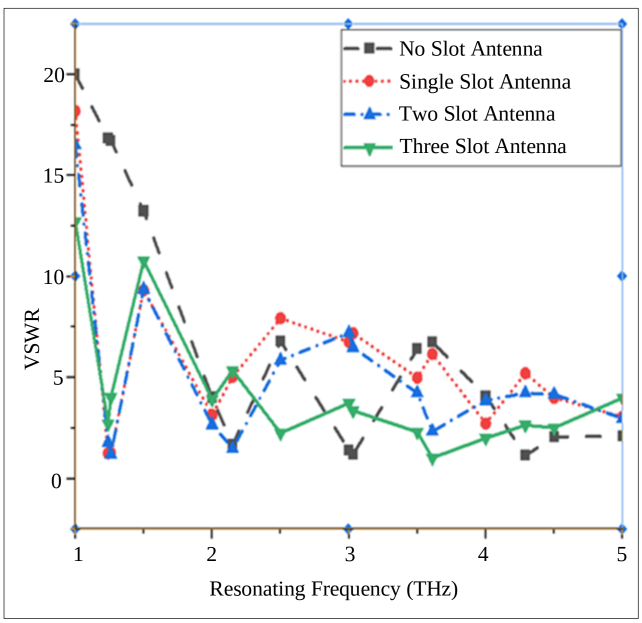

Fig. 4 Graph of VSWR versus resonating frequency of the triangular shaped antenna

Table 4. VSWR with and without slotted antenna

Sl No.	Triangular Antennas	Frequency (THz)	VSWR
1	No Slot	4.30	1.16
2	Single Slot	1.25	2.11
3	Double Slot	2.11	1.04
4	**Three Slot**	**3.16**	**1.03**

3.3. Electric and Magnetic Field

The electric field (E-field) and magnetic field (H-field) distributions are key for understanding the antenna's performance. Figures 5, 6, 7, and 8 show how high (red colour) and low (blue colour) intensity of electric field radiation are seen near antenna elements.

The E-field also defines how the voltage or electric potential varies spatially, influencing the radiation characteristics of antennas, waveguides, and other radio frequency components. The energy distribution of all the communicating antennas is stable in space.

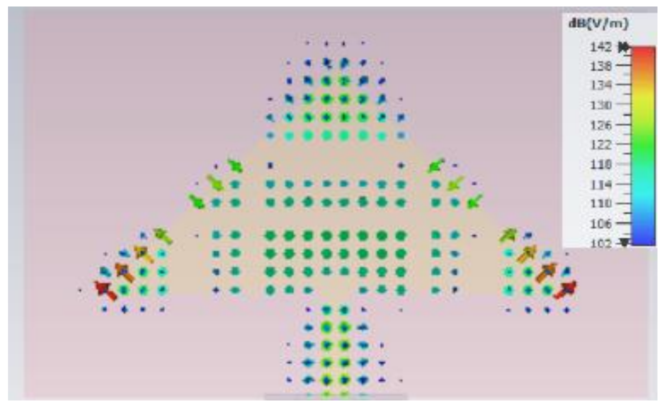

Fig. 5 E-field of no-slot antenna

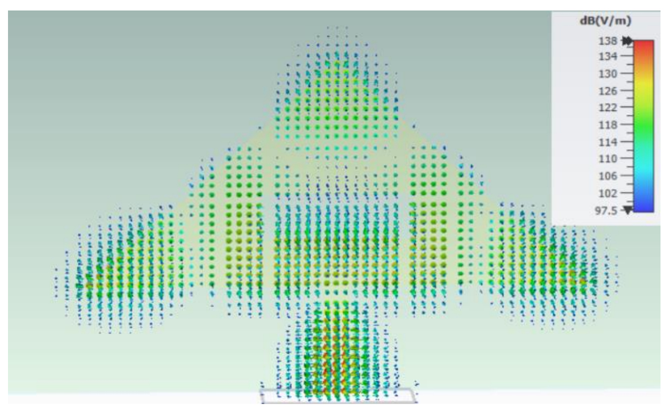

Fig. 6 E-field of single-slot antenna

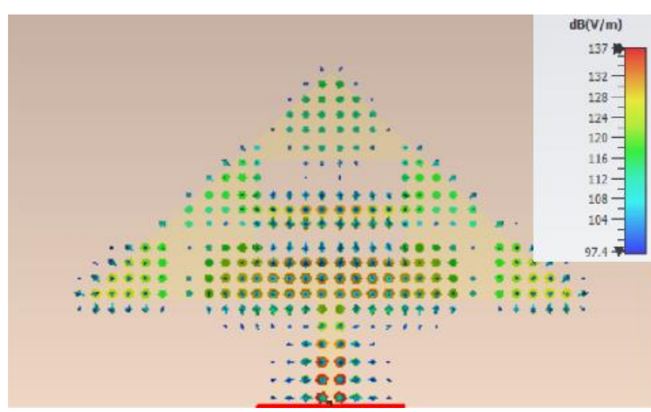

Fig. 7 E-field of double-slot antenna

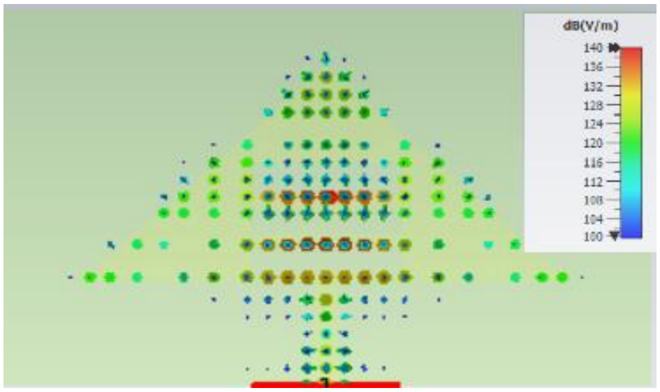

Fig. 8. E-field of three-slot antenna

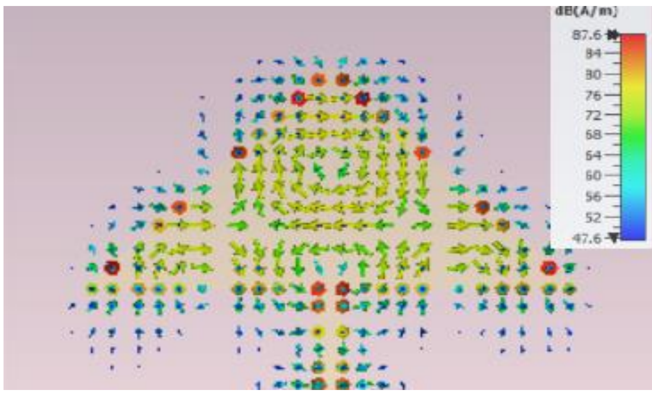

Fig. 9 H-field of no-slot antenna

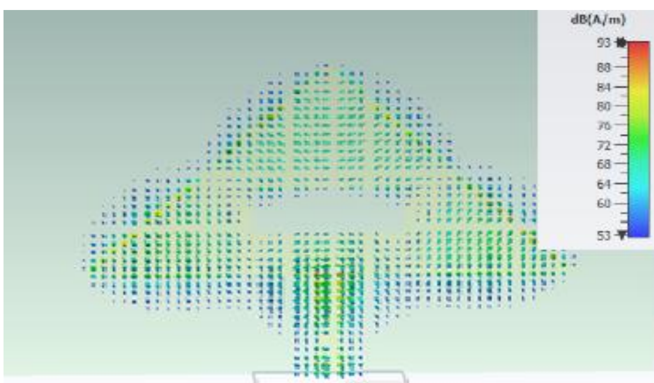

Fig. 10 H-field of single-slot antenna

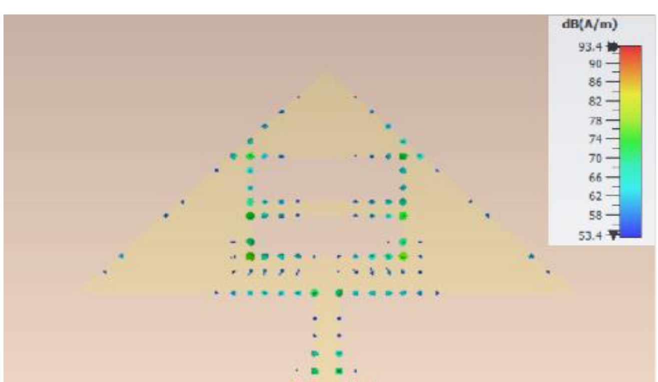

Fig. 11 H-field of double-slot antenna

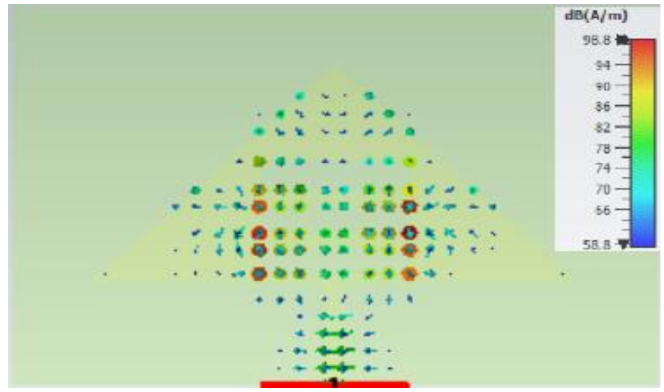

Fig. 12 H-Field of three-slot antenna

The magnetic field pattern in the near and far field will also reflect the antenna's radiation pattern, decreasing the field strength as you move away from the main lobe. Figures 9, 10, 11, and 12 show how magnetic field distribution occurs and how all the antennas successfully radiate the energy.

3.4. Surface Current

The surface current spreading on a 6G antenna is a main indicator of how well the antenna radiates and how efficiently it converts input power into electromagnetic waves, and it is measured in amperes per meter (A/m). Examining the surface current helps to understand the regions of the antenna that are most active in radiation and can help improve the design.

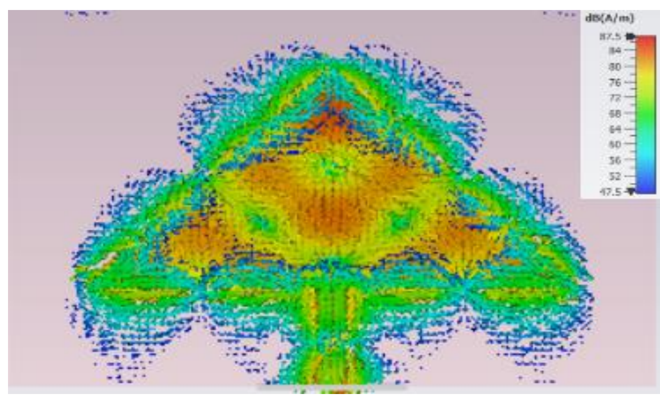

Fig. 13. Surface current of no-slot antenna

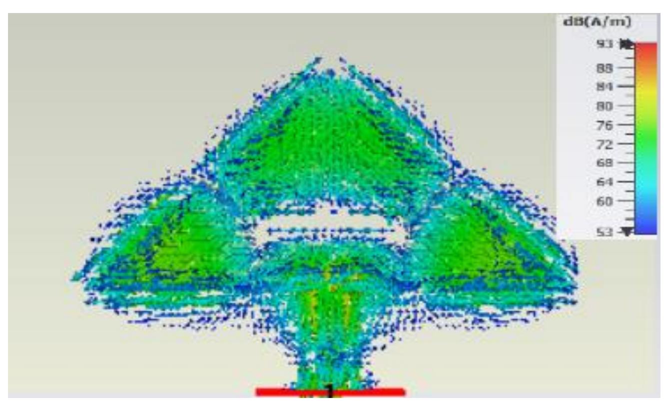

Fig. 14. Surface current of single-slot antenna

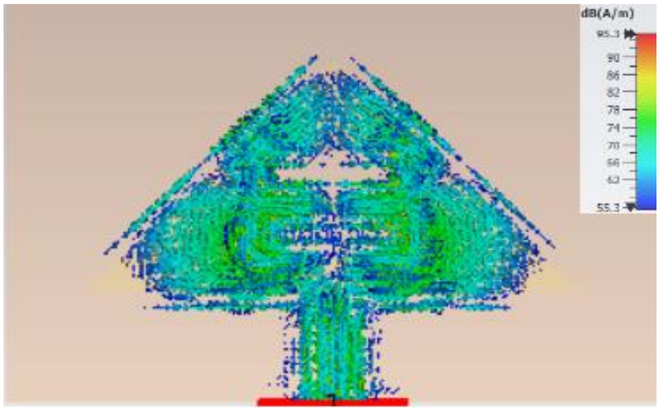

Fig. 15. Surface current of double-slot antenna

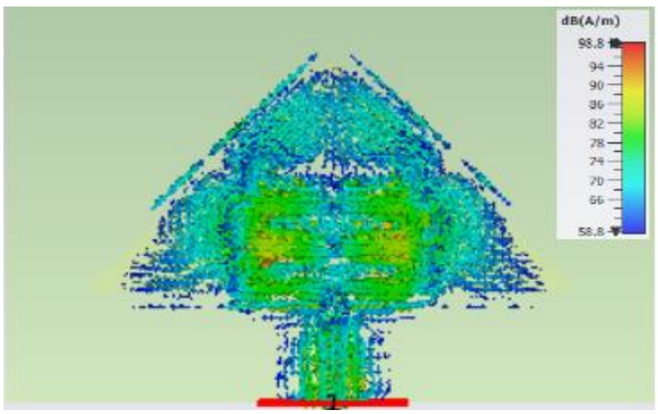

Fig. 16 Surface current of three-slot antenna

Figures 13, 14, 15, and 16 show how electromagnetic waves interrelate with conductors, antennas, and other RF components, as surface currents directly impact these devices' radiation, scattering, and absorption properties.

3.5. Far Field Region

In the microstrip 6G antenna design, the "far-field" or “Fraunhofer region” denotes the region far enough away from the antenna where the electromagnetic fields are radiating and whether it is directing energy as expected. This area is critical for analyzing the antenna’s radiation features, such as directivity, gain, radiation pattern, and efficiency. The radiation pattern describes how the antenna radiates energy into the surrounding space as a function of direction, and it is typically represented as a 2D or 3D plot.

The CST tool allows us to visualize the radiation pattern in polar (2D) and spherical (3D) coordinates. It gives insight into the main lobe, side lobes, and nulls of the radiation. The directivity of an antenna is a measure of how concentrated the radiated power is in a particular direction, and the directivity is calculated from the radiation pattern. The directivity of an antenna is mainly based on the antenna type, design goals, and application. Figures 17, 18, 19, and 20 show the directivity of the radiation pattern, angular width, and side lobe level, and it is measured in dBi (decibels relative to an isotropic radiator).

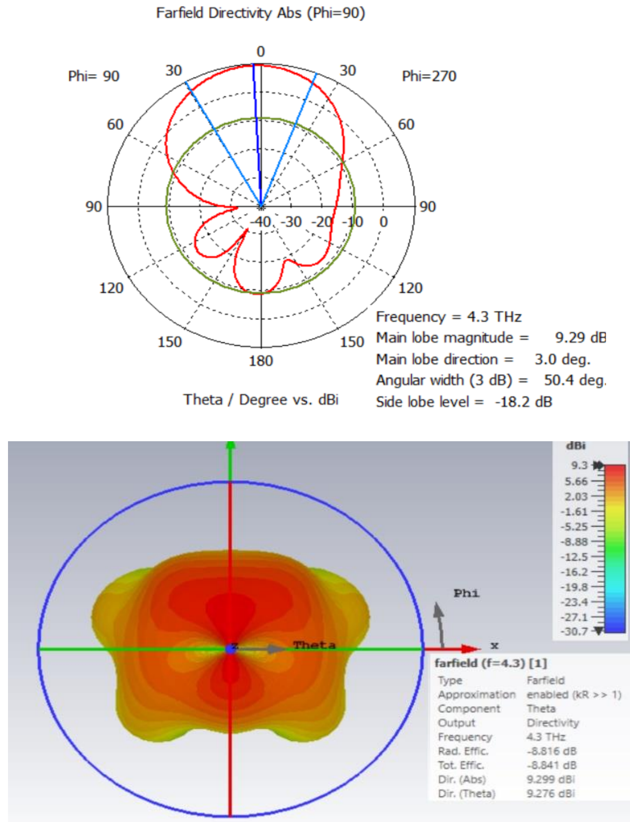

Fig. 17 Far field directivity of no-slot antenna

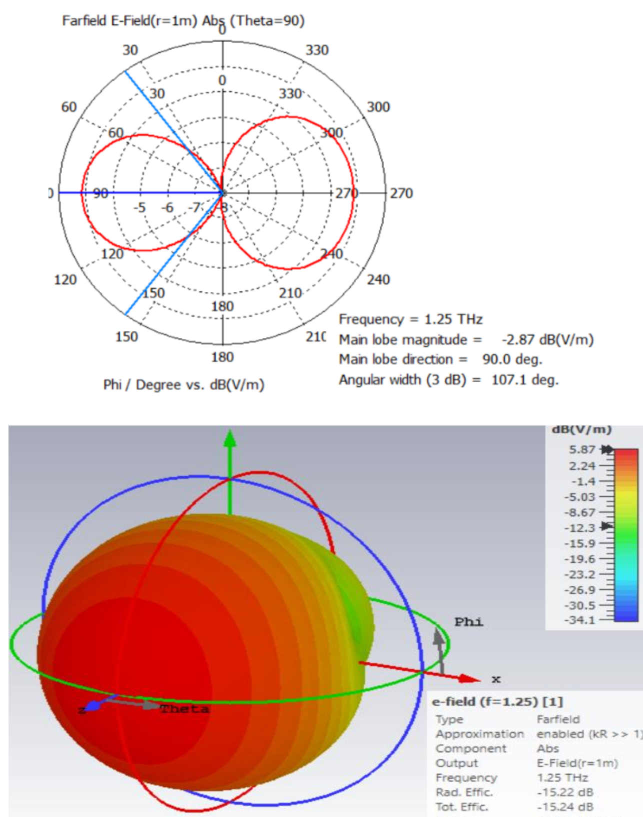

Fig. 18 Far field directivity of single-slot antenna

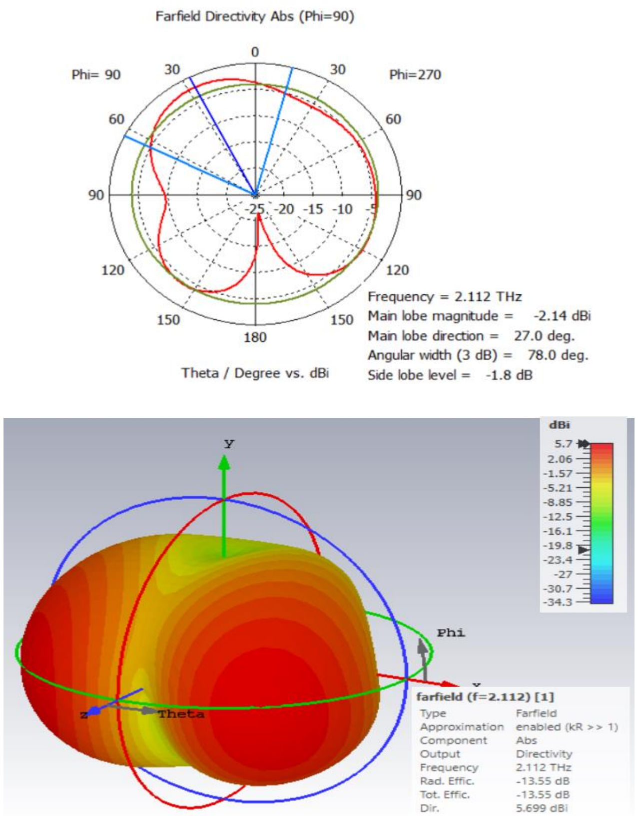

Fig. 19 Far field of double slot antenna

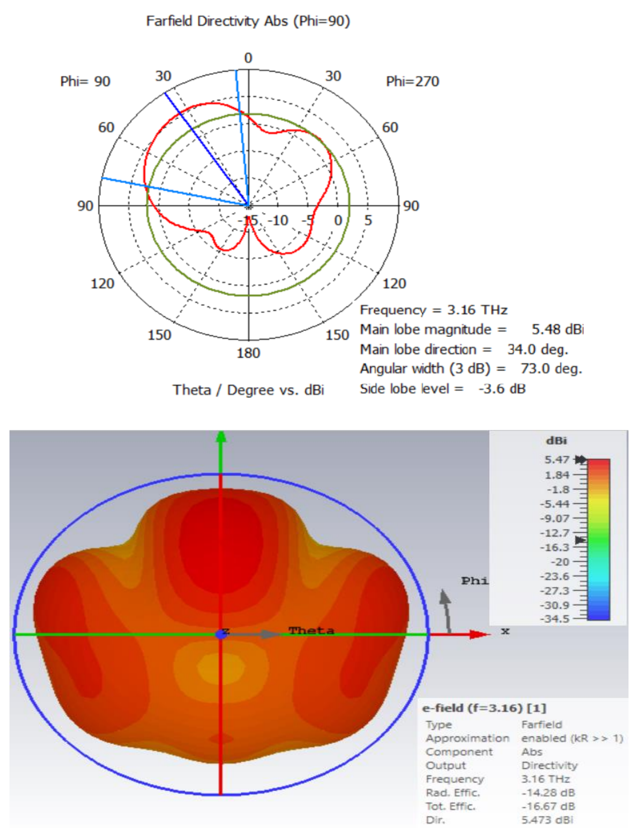

Fig. 20 Far field of three-slot antenna

Table 5. Directivity of with and without slot antennas

Sl No.	Triangular Antennas	Frequency (THz)	Directivity (dBi)	Gain (dB)
1	No Slot	4.30	3.30	5.59
2	Single Slot	1.25	6.34	5.51
3	Double Slot	2.11	5.69	7.38
4	**Three Slot**	**3.16**	**5.47**	**8.43**

Individual antenna types, e.g., patches or dipoles, typically have low directivity of 5 dBi to 10 dBi at terahertz frequencies. The antenna gain value is important due to the unique challenges of operating at such high frequencies. Terahertz frequencies typically range from 1 THz to 3 THz, and antennas in this range require high gain to overcome significant free-space path loss and atmospheric attenuation. However, individual patch antenna elements often exhibit lower gains, ranging from 5 dB to 10 dB.

4. Conclusion

In recent years, the antenna design for multi-band frequency has been critical because of its characteristics. The proposed triangular-shaped microstrip patch antennas are new and unique. In this paper, the proposed antennas highlight challenges such as wideband operation, miniaturized structure, return loss, gain, directivity, impedance matching, and beamforming.

The simulation results show the performances of all four antennas in Tables 3, 4, and 5. Among all four proposed 6G antennas, the triangular antenna with three slots operating with a 3.16 THz resonant frequency offers better performance in bandwidth, reduced size, low return loss, better directivity, and gain.

According to the results, the other antennas with no slot, a single slot, and a double slot also perform better to some extent. The gain of the proposed antennas can be further extended by increasing the number of patches with slots in the array structure.

Overall, the outcome of these antennas defines that they are appropriate for the terahertz 6G communication system. This work can further simulate different terahertz frequencies with different designs, materials, and antenna shapes. The practical implementation challenges will be systematically investigated, such as integration with wearable devices, power consumption, and durability under various environmental conditions (e.g., humidity, temperature, and physical strain).

These antennas can be future used in Wireless Body area Network (WBN) for healthcare applications, ensuring reliability, safety, and user comfort. Collaboration with healthcare professionals will also be considered to tailor the designs to specific medical use cases, such as remote patient monitoring or disease diagnosis.

References

[1] Tej Raj et al., "Advances in MIMO Antenna Design for 5G: A Comprehensive Review," *Sensors*, vol. 23, no. 14, pp. 1-34, 2023. [CrossRef] [Google Scholar] [Publisher Link]

[2] Shizhen Jia, and Hui Xu, "Two 5G Patch Antenna Designs for Millimeter-Wave," *2022 14th International Conference on Computer Research and Development (ICCRD)*, Shenzhen, China, pp. 378-387, 2022. [CrossRef] [Google Scholar] [Publisher Link]

[3] Amin Al Ka'bi, and Ali Mustafa, "Design of MIMO Antenna for Wideband THz Mobile Communications and Radio Engineering," *Journal of Telecommunication and Radio-Engineering*, vol. 83, no. 8, pp. 1-12, 2024. [CrossRef] [Google Scholar] [Publisher Link]

[4] Arselan Ashraf et al., "Advancements and Challenges in Scalable Modular Antenna Arrays for 5G Massive MIMO Networks," *IEEE Access*, vol. 12, pp. 57895-57916, 2024. [CrossRef] [Google Scholar] [Publisher Link]

[5] Josheena Gnanathickam, Gajula Thanusha, and Nesasudha Moses, "Design and Development of Microstrip Patch Antenna for 5G Application," *2023 International Conference on Computer Communication and Informatics (ICCCI)*, Coimbatore, India, pp. 1-4, 2023. [CrossRef] [Google Scholar] [Publisher Link]

[6] H.T. Chou et al., "Dual-Band Reflect Array Antennas Using Integrated Resonant and Non-Resonant Natures of Metallic Waveguide Elements at Millimeter Wave Frequencies," *Radio Science*, vol. 58, no. 1, pp. 1-13, 2023. [CrossRef] [Google Scholar] [Publisher Link]

[7] Giulia Buttazzoni et al., "A Beamforming Network for 5G/6G Multibeam Antennas Using the PCB Technology," *2023 17th European Conference on Antennas and Propagation (EuCAP)*, Florence, Italy, pp. 1-5, 2023. [CrossRef] [Google Scholar] [Publisher Link]

[8] Wei Hong, Zi-Jun Guo, and Zhang-Cheng Hao, "Seamless Integration Technology for Filtenna Toward 5G/6G Wireless Communications," *IEEE Open Journal of Antennas and Propagation*, vol. 5, no. 1, pp. 18-36, 2024.[CrossRef] [Google Scholar] [Publisher Link]

[9] Vishal Walia, Md Rashid Mahmood, and Vikas Maheshwari, "Sustainable Spectrum Sharing 5G Network Antenna Design for Smart City," *Journal of Autonomous Intelligence*, vol. 7, no. 4, pp. 1-8, 2024. [CrossRef] [Google Scholar] [Publisher Link]

[10] Hesham A. Mohamed et al., "Millimeter-Wave Antenna with Gain Improvement Utilizing Reflection FSS for 5G Networks," *IEEE Access*, vol. 10, pp. 73601-73609, 2022. [CrossRef] [Google Scholar] [Publisher Link]

[11] Angotu Saida, R.K. Yadav, and V.K. Sharma, "Analysis of LTE Based an Antenna Design for 5G Communications," *International and Journal on Recent and Innovation Trends in Computing and Communication*, vol. 11, no. 6, pp. 471-475, 2023. [CrossRef] [Google Scholar] [Publisher Link]

[12] Marwa M. El-Wazzan et al., "Compact and Integrated Microstrip Antenna Modules for mm-Wave and Microwave Bands Applications," *IEEE Access*, vol. 10, pp. 70724-70736, 2022. [CrossRef] [Google Scholar] [Publisher Link]

[13] Usha Sharma et al., "Design Challenges and Solutions of Multiband MIMO Antenna for 5G/6G Wireless Applications: A Comprehensive Review," *Progress in Electromagnetics Research*, vol. 104, pp. 69-89, 2023. [CrossRef] [Google Scholar] [Publisher Link]

[14] S. Kalpana, and S. Mangayarkarasi, "Design of Microstrip Based Millimeter Wave Antenna for 5G Applications," *2023 2nd International Conference on Smart Technologies and Systems for Next Generation Computing (ICSTSN)*, Villupuram, India, pp. 1-5, 2023. [CrossRef] [Google Scholar] [Publisher Link]

[15] Samrat Sadhu, Bhaskar Acharjee, and Sudip Mandal, "Design of Wideband Microstrip Patch Antenna at 38 GHz for 5G Network," *International Conference on Data Science and Communication*, Springer, Singapore, pp. 719-730, 2023. [CrossRef] [Google Scholar] [Publisher Link]

[16] Guo-Ping Gao et al., "A Compact Tri-Port MIMO Antenna with High Isolation for Broadside and Conical Radiation," *IEEE Internet of Things Journal*, 2024. [CrossRef] [Google Scholar] [Publisher Link]